Lilia Sabantina[1,2],
Lubos Hes[3],
José Rodríguez Mirasol[1],
Tomás Cordero[1],
Andrea Ehrmann[2,*]

Water Vapor Permeability through PAN Nanofiber Mat with Varying Membrane-Like Areas

DOI: 10.5604/01.3001.0012.7502

[1] University of Malaga, Andalucía Tech, Department of Chemical Engineering, 29010 Málaga, Spain

[2] Bielefeld University of Applied Sciences, Faculty of Engineering and Mathematics, Working Group of Textile Technologies, 33619 Bielefeld, Germany
* e-mail: andrea.ehrmann@fh-bielefeld.de

[3] Technical University of Liberec, 46117 Czech Republic

Abstract
Electrospinning can be used to create nanofiber mats from diverse polymers which can be used as filters etc. Depending on the spinning parameters, also nano-membranes, i.e. non-fibrous mats, can be produced as well as mixtures from both morphologies. The ratio of membrane to fibrous areas can be tailored by the distance between the high voltage electrode and substrate. Here the impact of the mat morphology on the water vapour permeability through polyacrylonitrile nanofiber mats with different membrane-like areas is shown, allowing for tailoring the permeability between 0.1 Pa · m²/W and more than 10 Pa · m²/W. In this way it is possible to create the finest filters as well as nearly impenetrable thin membranes with the same technology.

Key words: *electrospinning, water vapour permeability, polyacrylonitrile, nanofiber mat, nano-membrane.*

Introduction

Electrospinning is a technology allowing for the creation of fine fibers with diameters between some ten and several hundred nanometers, sometimes a few micrometers. The electrostatic forces in a strong electric field draw a molten or dissolved polymer to a substrate, at the same time stretching and drying the polymer so that the finest fibers are formed and finally placed on the substrate. Diverse polymers, polymer blends and other materials can be used to create such nanofiber mats [1-3], amongst which is a broad variety of biopolymers, as well as typical industrially used polymers such as polyacrylonitrile (PAN), polyamides, polyesters, etc.

Nanofibers created by electrospinning have round cross-sections in most cases, whose diameters can be changed by modifying the polymer solid content in the solution/melt as well as other spinning and solution parameters [4, 5]. Besides this typical form, flat ribbons can also be produced [6, 7]. Pure droplets [8] or combinations of droplets and fibers are also possible results of the electrospinning process [4, 9].

Finally it is possible to create mixtures of fibers and membranes or pure membranes. In a former project, the feasibility of creating mats with tailored fiber/membrane area ratios was investigated, especially for chitosan/poly(ethylene glycol) (PEG) blends, finding that the chitosan: PEG ratio was crucial for mat morphology [10, 11]. Another way to intentionally create membrane areas is adding surfactants to reduce the surface tension of the spinning solution and thus avoid fiber formation [12].

An interesting material for possible use in filters etc. is PAN, which is not water-soluble and can thus be utilised without a further stabilisation step. For PAN, by changing the distance between the high voltage electrode and substrate, the morphology can be varied from pure nanofibers for large distances to pure membranes for small distances [13]. This finding can be attributed to the flight time of the fibers – if this time is reduced, the solvent is not completely evaporated before the substrate is reached, and the still partly dissolved fibers can unite to finally form a fine membrane instead of single fibers.

This effect means not only that the distance chosen between the high voltage electrode and substrate is relevant for the resulting morphology, i.e. the ratio of membrane to nanofiber areas, but also that deviations from the middle of the substrate – where the distance to the high voltage electrode is smallest – to the borders can also be expected. However, in scientific literature only a few reports about examinations of this effect can be found. Niu *et al.*, e.g., calculated the influence of different fiber generator geometries, amongst which they also investigated cylinders with different diameters. They found that the electric field intensity in the middle area increased with a decreasing cylinder diameter, i.e. it should be highest for a thin wire, while at the same time the discrepancies along the whole substrate increased [14]. Wang *et*

Sabantina L, Hes L, Mirasol JR, Cordero T, Ehrmann A. Water Vapor Permeability through PAN Nanofiber Mat with Varying Membrane-Like Areas.
FIBRES & TEXTILES in Eastern Europe 2019; 27, 1(133): 12-15. **DOI:** 10.5604/01.3001.0012.7502

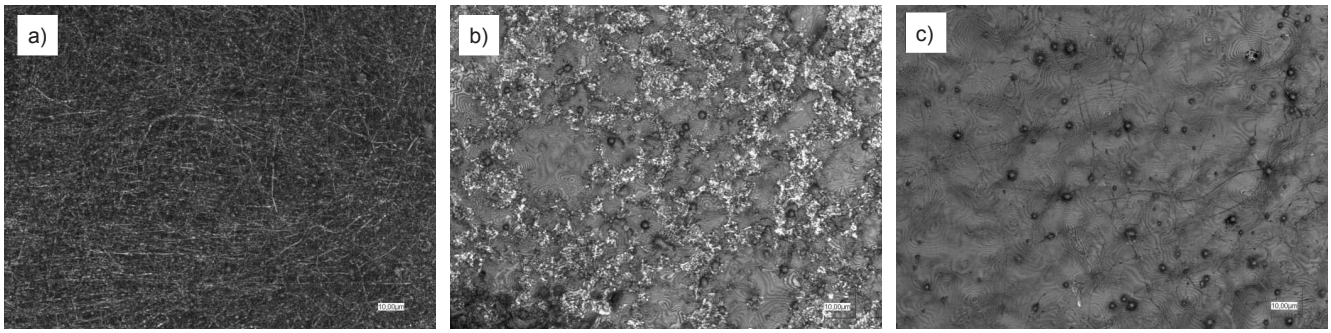

Figure 1. *Electrospun nanofiber mats prepared with an approx: a) 2 %, b) 68 % and c) 99.9 % membrane ratio. All scale bars have a length of 10 μm.*

al. used a simulation to optimise the electric field in a series of modelled designs, starting from a cylindrical spinneret [15]. Fractal spinnerets were optimised by simulations and found to achieve more homogeneous electric field distributions than recent needleless electrospinning technologies [16]. Earlier research concentrated on replacing single needle technology – which results in the most non-uniform electrical field distribution – by a flat spinneret to gain more uniform nanofiber mats [17]. Other simulations revealed that even along a cylinder used as a spinneret, the electric field was not constant, but concentrated along the cylinder ends [18].

The inhomogeneity of the electrospun nanofiber mat in terms of thickness, morphology, porosity and mechanical properties was also compared for stationary and dynamic collectors, showing that irrespective of the collector template design, there was a significant inhomogeneity for the stationary mode, which could be significantly improved by using the dynamic mode and a sophisticated template design [19]. Taking the capillary tubes in a multicapillary head into account, the electric field distribution was modelled and experimentally verified by measuring the transverse fiber dimensions and shape of the fiber cross-sections [20].

Generally a review article stated just recently that the pore diameters in different places of nanofiber mats are very unequal, making it necessary to investigate not only one or a few areas of the mat to detect its morphology, but several more points [21] This is understandable due to simulations showing the spatial variation of the electrostatic field for one electrode [22-25] or multiple capillaries [26-27] as well as to the above-mentioned models of diverse needleless geometries. Taking into account these findings, we took care to correlate properties not of complete nanofiber mats but of specific areas in which the correlated measurements were taken.

In this paper, the water vapour resistance of mats with varying morphologies for pure nanofibers and membranes was examined. Although this property is essential for many applications, especially for filtration, it has been only scarcely investigated for nanofiber mats. Recently two methods (dry cup method and tube method) of measuring water vapour diffusion through a polyurethane nanofiber mat were compared, without using these methods to examine the influence of spinning parameters on water vapour permeability [28]. The water vapour permeability of an electrospun nanofiber mat was not significantly altered by polyurethane coating [29]. For a membrane consisting of hollow fibers, water vapour permeability was investigated in dependence on the operating temperature and other operating parameters [30]. Linking the inter-fiber junction points after the spinning process by exposing the nanofiber mat to a solvent vapour was shown to not significantly reduce the water vapour permeability [31]. The effect of fluorination on water vapour permeation was studied for polyurethane nanofiber mats [32]. The influence of modification of the nanofiber web density on water resistance combined with water vapour and air permeability was investigated for layered fabric structures consisting of electrospun nanofiber mats and different substrates [33]. However, investigations of the transition between the nanofiber mat and the membrane in terms of water vapour permeability cannot be found in literature.

Materials and methods

The wire-based electrospinning machine "Nanospider Lab" (Elmarco, Czech Republic) was used for electrospinning, applying a high voltage of 80 kV, nozzle diameter of 0.9 mm and carriage speed of 150 mm/s during a spinning time of 5 min. Since the voltage strongly influences the nanofiber diameters and lengths [13], it was kept constant to avoid possible modifications of the water vapour permeability due to modified pore diameters. Similarly, changing the nozzle diameter, carriage speed or spinning time would influence the nanofiber mat thickness and correspondingly again the water vapour permeability, which was avoided in this test series, concentrating on the influence of membrane/nanofiber creation. The distance between the high voltage electrode and the middle of the substrate was varied between 120 mm and 240 mm (the maximally possible values).

A PAN solution for spinning was prepared with 14 % solid content in DMSO (dimethyl sulfoxide) by stirring for 2 hours at room temperature. This concentration was found ideal in previous tests to avoid clogging of the nozzle as well as electrospraying, as opposed to electrospinning.

Investigation of the nanofiber mat morphologies was performed by means of a confocal laser scanning microscope (CLSM) VK-9000 (Keyence) with a nominal magnification of 2000 x, using three areas per sample.

A Permetest skin model (built by Sensora Textile Measuring Instruments and Consulting, Czech Republic) was used to measure the water vapour resistance [34] in three areas per sample.

The software ImageJ 1.51j8 (from National Institutes of Health, Bethesda (MD), USA) was applied to determine the ratio of membrane/nanofiber areas in CLSM images.

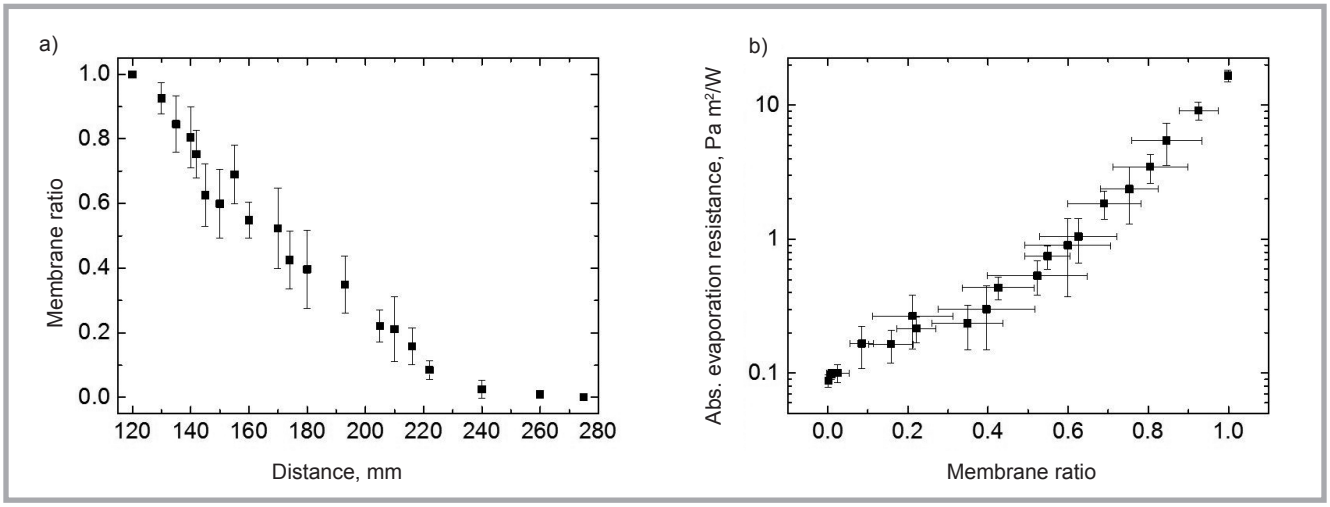

Figure 2. *Correlation between: a) membrane ratio and electrode-substrate distance and b) absolute evaporation resistance and membrane ratio (i.e. the membrane area divided by the whole area) in PAN nanofiber mats.*

Results and discussion

Varying the distance between the electrodes results in nearly perfect nanofiber mats for the largest possible distance (***Figure 1.a***), nearly complete membranes without holes for the smallest possible distance (***Figure 1.c***) and diverse mixtures of both morphologies for intermediate distances (***Figure 1.b***). Apparently it is possible to tailor the desired fiber-to-membrane ratio by varying this parameter.

Figure 2.a depicts the influence of the electrode-substrate distance on the membrane ratio of the nanofiber mats. Besides measurements in the middle of the sample, i.e. on the direct line between both electrode wires, measurements along the borders were made for which the distances between the substrate and high voltage electrode were calculated along the direct connection lines between the respective positions on the substrate and wire. Although the newly formed nanofibers can be expected to impinge on the substrate under different angles and despite electric fields being known to vary along the substrate area, combining all these measurements in one correlation works unexpectedly well.

An approximately linear decrease in the membrane ratio with increasing distance is visible until at ~ 230 cm distance the membrane areas vanish nearly completely. It should be mentioned that depending on the relative humidity in the spinning chamber and the solid content in the spinning solution, small membrane-like areas are often visible in "pure" nanofiber mats (cf. ***Figure 1.a***), so that the membrane area for a typical electrospinning situation is often not exactly zero.

Figure 2.b shows measurements of the absolute evaporation resistance and membrane part of the nanofiber mats, as determined from 3 CLSM images per sample. Please note that the y-axis is scaled logarithmically. Generally a linear correlation can be estimated in this graph, indicating an exponential correlation between the absolute evaporation resistance and membrane ratio. Nevertheless it must be mentioned that while the absolute evaporation resistance of most samples has relatively small standard deviations, evaluations of the CLSM images with respect to the membrane ratios show partly large error bars, especially for membrane fractions around 0.2-0.8. This finding can be attributed to partly irregular nanofiber mats, exhibiting differing morphologies on the small dimensions visible in each CLSM image.

Conclusions

In conclusion, PAN nano-mats with different ratios of nanofibers and membrane-like areas were prepared. The membrane:nanofiber ratio could be tailored by modifying the distance between the high voltage electrode and substrate. Measuring the water vapour permeability showed an approximately exponential correlation between the absolute evaporation resistance and membrane ratio. The water vapour permeability could be varied by more than two orders of magnitude, showing possibilities to tailor this value by modifying the electrospinning parameters.

Acknowledgements

The authors gratefully acknowledge the program FH Basis of the German federal region of North Rhine-Westphalia for funding the "Nanospider Lab" and the Erasmus+ program of the European Union.

References

1. Kenawy ER, Layman JM, Watkins JR, Bowlin GL, Matthews JA, Simpson DG and Wnek GE. Electrospinning of poly(ethylene-co-vinyl alcohol) fibers, Biomaterials. 2003; 24(6): 907-913.
2. Deitzel JM, Kleinmeyer JD, Hirvonen JK, and Beck Tan NC. Controlled deposition of electrospun poly(ethylene oxide) fibers. *Polymer* 2001 42(19): 8163-8170.
3. Reneker DH and Chun I. Nanometre diameter fibres of polymer, produced by electrospinning. *Nanotechnology* 1996; 7: 216-223.
4. Larrondo L, Manley RSJ. Electrostatic fiber spinning from polymer melts. I. Experimental observations on fiber formation and properties. *J Polym Sci Polym Phys Ed* 1981; 19: 909-920.
5. Grothe T, Brikmann J, Meissner H, Ehrmann A. Needleless electrospinning of poly(ethylene oxide). *Materials Science* 2017; 23(4): 342-349.
6. Koombhongse S, Liu W, Reneker DH. Flat ribbons and other shapes by electrospinning. *J Polym Sci, Polym Phys Ed* 2001; 39: 2598-2606.
7. Frenot A, Chronakis IS. Polymer nanofibers assembled by electrospinning. *Current Opinion in Colloid and Interface Science* 2003; 8: 64-75.
8. Grothe T, Großerhode C, Hauser T, Kern P, Stute K, Ehrmann A. Needleless electrospinning of PEO nanofiber mats. *Advances in Engineering Research* 2017; 102: 54-58.
9. Fong H, Chun I, Reneker DH. Beaded nanofibers formed during electrospinning. *Polymer* 1999; 40: 4585-4592.

10. Grimmelsmann N, Homburg SV, Ehrmann A. Electrospinning chitosan blends for nonwovens with morphologies between nanofiber mat and membrane. *IOP Conference Series: Materials Science and Engineering* 2017; 213, no. 012007.
11. Grimmelsmann N, Homburg SV, Ehrmann A. Needleless electrospinning of pure and blended chitosan. *IOP Conference Series: Materials Science and Engineering* 2017; 225, no. 012098.
12. Yalcinkaya F, Yalcinkaya B, Jirsak O. Dependent and Independent Parameters of Needleless Electrospinning, Electrospinning – Material, Techniques and Biomedical Applications 2016; pp. 67-93.
13. Sabantina L, Mirasol JR, Cordero T, Finsterbusch K and Ehrmann A. Investigation of Needleless Electrospun PAN Nanofiber Mats. *AIP Conference Proceedings* 2017; 1952, 020085.
14. Niu HT, Wang XG, Lin T. Needleless electrospinning: influences of fibre generator geometry. *Journal of the Textile Institute* 2012; 103: 787-794.
15. Wang W, Qiang W, Dai HC. Impact Mechanisms of Needleless Electrospinning Spinneret Geometry on Electric Field Distribution Regularities. *Chemical Journal of Chinese Universities* 2017; 38: 982-989.
16. Yang WX, Liu YB, Zhang LG, Cao H, Wang Y, Yao JB. Optimal spinneret layout in Von Koch curves of fractal theory based needleless electrospinning process. *AIP Advances* 2016; 6, 065223.
17. Zhou F-L, Gong R-H, Porat I. Needle and Needleless Electrospinning for Nanofibers. *Journal of Applied Polymer Science* 2010; vol 115: 2591-2598.
18. Niu HT, Lin T, Wang XG. Needleless Electrospinning. I. A Comparison of Cylinder and Disk Nozzles. *Journal of Applied Polymer Science* 2009; 114: 3524-3530.
19. Pathalamuthu P, Shahana ST, Nivedha U, Siddharthan A, Giridev VR. *FIBRES & TEXTILES in Eastern Europe* 2017; 25, 3(123): 53-61. Nr DOI: 10.5604/01.3001.0010.1689.
20. Krucinska I, Komisarczyk A, Chrzanowski M, Gliscinska E, Wrzosek H., Electrostatic Field in Electrospinning with a Multicapillary Head – Modelling and Experiment. *FIBRES & TEXTILEs in Eastern Europe* 2009; 17, 3(74): 38-44.
21. Kleivaite V, Milasius R. Electrospinning – 100 years of investigations and still open questions of web structure estimination. *AUTEX Research Journal* 2018, *online first*.
22. Carnell LS, Siochi EJ, Wincheski RA, Holloway NM, Clark RL. Electric field effects on fiber alignment using an auxiliary electrode during electrospinning. *Scripta Materialia* 2009; 60: 359-361.
23. Thompson CJ, Chase GG, Yarin AL, Reneker DH. Effects of parameters on nanofiber diameter determined from electrospinning model. *Polymer* 2007; 487: 6913-6922.
24. Zheng Y, Xie S, Zeng Y. Electric field distribution and jet motion in electrospinning process: from needle to hole. *Journal of Materials Science* 2013; 48: 6647-6655.
25. Yang Y, Jia Z, Liu J, Li Q, Hou L, Wang L, Guan Z. Effect of electric field distribution uniformity on electrospinning. *Journal of Applied Physics* 2008; 103, 104307.
26. Theron SA, Yarin AL, Zussman E, Kroll E. Multiple jets in electrospinning: experiment and modeling. *Polymer* 2005; 46: 2889-2899.
27. Firych-Nowacka A, Smólka K, Wiak S, Gliscinska E, Kricinska I, Chrzanowski M. 3-dimensional computer model of electrospinning multicapillary unit used for electrostatic field analysis. *Open Physics* 2017; 15: 1049-1054.
28. Cernohorsky M, Semerak P, Ticha P, Havrlik M. Measuring of Water Vapour Diffusion of Nanofibre Textiles, 8th International Conference on Nanomaterials – Research & Application 2017; 319-323.
29. Hong KA, Yoo HS, Kim E. Effect of waterborne polyurethane coating on the durability and breathable waterproofing of electrospun nanofiber web-laminated fabrics. *Text. Res. J.* 2015; 85(2): 160-170.
30. Sun AC, Kosar W, Zhang YF, Feng XS. Vacuum membrane distillation for desalination of water using hollow fiber membranes. *Journal of Membrane Science* 2014; 455: 131-142.
31. Huang L, Manickam SS, McCutcheon JR. Increasing strength of electrospun nanofiber membranes for water filtration using solvent vapor. *Journal of Membrane Science* 2013; 436: 213-220.
32. Shimada N, Mori T, Ito A, Yamaguchi S, Nakane K, Haraguchi M, Ozawa M, Ogata N., Structure and Physical Properties of Polyurethane/Fluorinated Hyper Branched Polymer Nanofiber Mat, Sen-I Gakkaishi 2012; 68(10): 269-275.
33. Yoon B, Lee S. Designing Waterproof Breathable Materials Based on Electrospun Nanofibers and Assessing the Performance Characteristics. *Fibers and Polymers* 2011; 12(1): 57-64.
34. Hes L. Araujo M. Simulation of the Effect of Air Gaps between the Skin and a Wet Fabric on Resulting Cooling Flow. *Textile Research Journal* 2010; 80: 1488-1497.

❑ ***Received 04.05.2018 Reviewed 24.08.2018***